We are IntechOpen, the world's leading publisher of Open Access books Built by scientists, for scientists

6,900
Open access books available

185,000
International authors and editors

200M
Downloads

Our authors are among the

154
Countries delivered to

TOP 1%
most cited scientists

12.2%
Contributors from top 500 universities



WEB OF SCIENCE™

Selection of our books indexed in the Book Citation Index in Web of Science™ Core Collection (BKCI)

Interested in publishing with us?
Contact book.department@intechopen.com

Numbers displayed above are based on latest data collected.
For more information visit www.intechopen.com



Chapter

Antenna Pattern Multiplexing for Enhancing Path Diversity

Masato Saito

Abstract

In this chapter, we show the concept of antenna pattern multiplexing (APM), which enhances path diversity gain and antenna pattern diversity reception in multipath rich fading environment. We discuss the types of antennas that achieve the APM, i.e., generating time-varying antenna pattern and the benefits of reducing antenna size and hardware cost. When electronically steerable passive array radiator (ESPAR) antenna is used, the benefits can be maximised. A model of receiving process is proposed for analysing the ergodic capacity of multiple-input multiple-output (MIMO) systems using APM. We derive a model of received signals to analyse the system performance. The received signal in matrix form includes an equivalent channel matrix, which is a product of antenna pattern matrix, the channel coefficient vector for each output. Numerical results in terms of ergodic capacity show the comparable performances of the proposed MIMO with APM to the conventional MIMO systems; in particular, the number of arrival paths and the number of antenna pattern are sufficiently large. Also the ergodic capacity can be equivalent to that of the conventional MIMO systems when the average SNR per antenna pattern is constant among the virtual antennas.

Keywords: antenna pattern multiplexing, path diversity, single-input multiple-output, multiple-input multiple-output, capacity, multipath fading

1. Introduction

Multiple-input multiple-output (MIMO) systems have attracted much attention as a means to improve the capacity of wireless communications by increasing the number of antennas. However, implementing multiple antennas can be a problem, particularly in mobile terminals due to their space limitation. In this study, we focus on array antennas at the receiver to enhance the capacity.

To resolve the problem, several methods have been proposed to achieve multiple separate received signal components by using a single radio frequency (RF) front-end with electronically steerable passive array radiator (ESPAR) antennas [1]. The modulated scattering array antenna was proposed for diversity and MIMO receivers [2–6]. The antenna consists of an antenna element for receiving signals and several modulated scattering elements (MSEs) like ESPAR antennas. The impedance of an MSE can be modulated or changed by with an applied sinusoidal voltage of frequency f_s to the variable reactance element connected to the MSEs. Then, the antenna patterns can vary also in a sinusoidal manner and can make the received signal frequency-shift by $\pm f_s$. The frequency-shifted components can be used for

IntechOpen

diversity reception. The virtually rotating antenna was proposed also to diversify the received signal components in the frequency domain [7, 8]. The principle of setting diversity branches in this domain is similar to that of the modulated scattering array antenna. In the rotating antenna, a combination of reactance values, which generates a desired antenna pattern, is applied sequentially to the multiple reactance elements of the antenna to rotationally change the directivity of the antenna. Also investigated was an ESPAR antenna based on the diversity receiver whose antenna patterns are time variable in a sinusoidal manner and are suitable for the MIMO-orthogonal frequency-division multiplexing (OFDM) receiver [9]. Other researches have been studied on diversity and MIMO receivers with ESPAR antennas having periodically variable antenna patterns by both theoretical and experimental investigations [10–14]. They also investigated the reactance time sequence, which generates sinusoidal antenna patterns with suppressed higher-order harmonics [15, 16].

In the studies shown above, it can be seen that, instead of using a fixed antenna pattern that may satisfy some criteria, they constantly changed the antenna pattern to generate multiple received signal components in the frequency domain. In this study, we propose a concept of antenna pattern multiplexing (APM) for setting multiple virtual antennas at the same location without additional physical antenna elements. Since the proposed APM also periodically varies antenna patterns to build multiple diversity branches or virtual antennas, it may be possible to consider the APM as a generalised method of the previously mentioned related studies. In APM, instead of sinusoidal waveforms or a sum of sinusoidal waveforms with different frequencies, we apply the sum of a set of orthogonal code sequences as the waveform to change antenna patterns. Therefore, the received signal can be separated into code domains to exploit path diversity instead of using only the narrow frequency domain, which is the case for the previous studies.

We introduce an antenna pattern matrix that consists of coefficients for each code sequence for each direction of received paths. With the matrix, we can derive the received signals of MIMO systems that use APM-based receivers in a form similar to the signals of the conventional MIMO systems. The ergodic capacity for the MIMO systems with APM technique is also derived[1]. Numerical results show that the capacity can be improved by increasing the number of arrival paths and the number of virtual antennas when the coefficients of APM are randomly distributed.

2. Types of antennas to achieve APM

Before mathematically analysing APM, we discuss the antennas that could realise the proposed APM concept. In APM, several antenna patterns, which are orthogonal to each other in time domain, should be multiplexed in similar manner to code-division multiplexing (CDM) or OFDM. To do so, it is essential that such antennas can generate time-varying antenna patterns. As such antennas, we consider array antennas or ESPAR antennas are good candidates because both antennas can change the antenna pattern from moment to moment.

We show a conceptual figure illustrating conventional array antenna, array antenna with APM, and ESPAR antenna with APM from left to right for comparative purposes in **Figure 1**. In the figure, we set the number of antenna elements at three as an example. Each antenna model consists of four parts: antenna elements,

[1] A part of the derivation is given in the our previous papers for limited cases of antenna pattern multiplexing [11, 17].

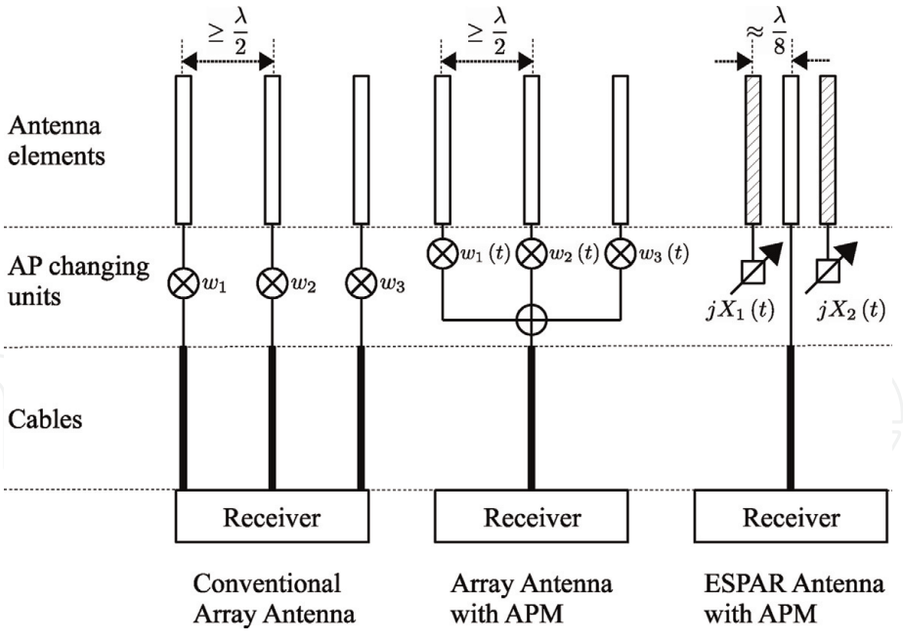


Figure 1.
The receiver models employing the conventional array antenna, array antenna with APM, and ESPAR antenna with APM of three antenna elements.

antenna pattern hanging units, cables between antenna elements and receivers, and receivers which receive signals through the cables.

In the part of antenna elements, the array antennas have three antenna elements connected to receivers, while ESPAR antenna has an element connected to the corresponding receiver and two parasitic elements which are connected to variable reactance components. In the figure, the shaded elements in ESPAR antenna show parasitic elements. In this part, the distance between neighbouring elements should be more than a half wavelength $\lambda/2$ for array antennas to reduce the correlation between the received signals obtained by the elements. On the other hand, since ESPAR antennas form antenna patterns by exploiting mutual coupling between antenna elements, the neighbouring elements need to be sufficiently close to each other. A study on ESPAR antenna with six parasitic elements describes that $\lambda/4$ is an appropriate distance [18]. In our previous work on two-element ESPAR antenna, appropriate distances between the elements are around $\lambda/8$ [16]. Hence, ESPAR antennas can reduce the space required for antenna elements less than a half of the space of array antennas in the case of three antenna elements. The increase in the number of antenna elements provides more gains in terms of reducing antenna sizes for ESPAR antennas.

The antenna elements are connected to AP changing units, which are weight multiplication for array antennas and variable reactance elements (VREs) for ESPAR antennas. In the conventional array antenna, constant weights w_1, w_2, and w_3 are multiplied to form an antenna pattern based on a criteria such as maximising the signal-to-interference-plus-noise ratio (SINR) or minimising the interference. In array antenna with APM, the weights are functions of time $w_1(t)$, $w_2(t)$, and $w_3(t)$, which form multiplexed AP and make the received signals travelling through antenna elements separable. Thus, we can add the signals and carry them to the receiver by a single cable. That is, the array antenna with APM can reduce the number of cables between antenna elements and the receiver and decrease their calibration cost. Since the parasitic elements do not connect to the receiver in ESPAR antenna, the cable cost can be also minimised. In ESPAR antenna, the antenna pattern or the directivity can be changed by the reactance values contributed by the parasitic elements. The reactance values of VREs can be changed by the

voltage applying to the VREs. Thus, multiplexed antenna patterns can be generated by changing the reactance values $jX_1(t)$ and $jX_2(t)$ which are both time-varying functions. Since the relationship between reactance values and generated antenna patterns is nonlinear, even two reactance functions can make several or more than three multiplexed antenna patterns.

Note that, in this study, the objective of varying the weights of the antennas is not to control the antenna pattern or form a pattern that satisfies some criteria. We need to simply have the functionality of periodically time-varying antenna patterns.

As can be seen from the figure, by ESPAR antennas, we can reduce the size related to antenna elements and the number of cables. Hence, we have selected the ESPAR antennas as a good candidate for utilising APM [10–13, 15, 16]. However, one of the problems relevant to using ESPAR antennas is in its difficulty of designing antenna patterns and time-varying voltage waveform applying to VREs. The difficulty comes from the nonlinear processes of the conversions from voltage to reactance and from reactance to antenna pattern and their time-varying properties. Therefore, to find the optimal set of voltage waveform applying to VREs is an open problem.

3. Modelling of antenna pattern multiplexing

In this section, we build a model of the receiver with APM and mathematically derive the received signals in MIMO applications.

3.1 Signals to change antenna pattern

As we mentioned in the previous section, the antenna patterns can be changed by applying periodically time variable voltages to the VREs connected to parasitic antenna elements. Since the applied voltages are periodic function of time, we assume that the appeared antenna patterns are also periodic functions of time.

We define a periodic function of time, $a_m(t)$, whose period is T_s. The function is assumed to be the weight for m-th antenna element for array antenna implementation and the reactance values of m-th VREs for ESPAR antenna implementation (see **Figure 1**). The function for a duration of the period $0 \le t < T_s$ is given by

$$a_m(t) = \sum_{k=1}^{N_a} b_{m,k} \cdot f_k(t), \tag{1}$$

where $f_k(t)$ is the k-th function of a set of N_a orthonormal functions and $b_{m,k}$ is a complex-valued coefficient of $f_k(t)$ for m-th element. Since the functions $f_k(t)$ are orthogonal to each other, they have the following property:

$$\frac{1}{T_s}\int_0^{T_s} f_k(t) \cdot f_l^*(t)\mathrm{d}t = \begin{cases} 1 & (k = l) \\ 0 & (k \neq l) \end{cases} \tag{2}$$

where $f_l^*(t)$ is the complex conjugate of $f_l(t)$. From the orthogonality shown in Eq. (2), we can derive another property for $k = l$ and assume a property for $k \neq l$ as

$$f_k(t) \cdot f_l^*(t) = \begin{cases} 1 & (k = l) \\ \exp\{j\Theta(t)\} & (k \neq l) \end{cases}, \tag{3}$$

where $\Theta(t)$ is a uniform random process in the interval $[0, 2\pi)$. The conventional APM methods use the DC and sinusoids of one or several frequencies as $f_k(t)$ in Eq. (1). In comparison, in this study, we consider the function $f_k(t)$ to be a signal that is spread by using the spreading code sequence used in direct-sequence spread spectrum (DSSS) systems or code-division multiple access (CDMA) systems. Thus, we assume the function $f_k(t)$ can be expressed as

$$f_k(t) = \sum_{l=1}^{N_c} c_{lk} \cdot g(t - (l-1)T_c), \tag{4}$$

where c_{lk} is the l-th chip of the waveform; $f_k(t)$ is assumed to have a complex value with a constant amplitude, $|c_{lk}| = 1/\sqrt{N_c}$; N_c is the number of chips in a period T_s; and $g(t)$ is the pulse waveform of a chip. In this paper, we assume that $g(t)$ is a rectangular pulse with duration T_c for simplicity. That is, $g(t)$ is shown as follows:

$$g(t) = \begin{cases} 1 & (0 \le t < T_c) \\ 0 & \text{otherwise} \end{cases} \tag{5}$$

The product of two functions in Eq. (3) for $0 \le t < T_s$ can be rewritten as follows:

$$f_k(t) \cdot f_l^*(t) = \sum_{m=1}^{N_c} c_{mk} \cdot c_{ml}^* \cdot g(t - (m-1)T_c) \cdot g^*(t - (m-1)T_c) \tag{6}$$

$$= \begin{cases} 1 & (k = l) \\ \sum_{m=1}^{N_c} c_{mk} \cdot c_{ml}^* \cdot g(t - (m-1)T_c) & (k \ne l) \end{cases} \tag{7}$$

As we can see from Eq. (7), the product can be shown by the product of only chips consisting of $f_k(t)$ and $f_l(t)$. Then, we consider a discrete time expression of $f_k(t)$ by introducing vector $\boldsymbol{c}_k$ whose components are the chips of $f_k(t)$. The vector can be given as

$$\boldsymbol{c}_k = (c_{1k} \;\; c_{2k} \;\; \cdots \;\; c_{N_c k})^{\mathrm{T}}, \tag{8}$$

where $^{\mathrm{T}}$ is a transpose operator. Then, we obtain a code matrix, C, by aligning the vectors as follows:

$$C = (\boldsymbol{c}_1 \quad \boldsymbol{c}_2 \quad \cdots \quad \boldsymbol{c}_{N_a}) \tag{9}$$

$$= \begin{pmatrix} c_{11} & c_{12} & \cdots & c_{1N_a} \\ c_{21} & c_{22} & \cdots & c_{2N_a} \\ \vdots & \vdots & \ddots & \vdots \\ c_{N_c 1} & c_{N_c 2} & \cdots & c_{N_c N_a} \end{pmatrix} \tag{10}$$

Since the orthogonality between two functions shown in Eq. (2) is satisfied, the following property of C can be derived:

$$C^{\mathrm{H}} C = I_{N_a} \tag{11}$$

where $^{\mathrm{H}}$ is an Hermitian transpose operator and I_{N_a} is the identity matrix of size $N_a \times N_a$.

The waveform $a_m(t)$ of Eq. (1) can be shown in a discrete time expression in matrix form as $C\boldsymbol{b}$ by setting a vector, $\boldsymbol{b} = (b_0 \;\; b_1 \cdots b_{N_a})^T$.

3.2 Received signals at receiver with APM

In the proposed APM, we apply signal $a_m(t)$ given in Eq. (1) to the antenna pattern changing units. Here, we assume that the mapping from the signals $a_m(t)$ to the antenna patterns is a linear map[2]. In other words, the generated antenna patterns can be shown in a linear combination of $f_l(t)$ for $l = 1, ..., N_a$.

Then, we consider the antenna pattern for a given direction. Suppose that a ball surrounds the entire receive antenna. On the ball, the p-th received signal path sent by l-th transmit antenna arrives at point $\left(\phi_{lp}, \theta_{lp}\right)$, where ϕ_{lp} is an azimuth and θ_{lp} is an elevation from the origin of the ball, respectively. We assume that a periodically time-varying far-field antenna pattern, $d_{lp}\left(\phi_{lp}, \theta_{lp}, t\right)$, which the arrival path experiences, in an equivalent baseband expression can be given as

$$d_{lp}\left(\phi_{lp}, \theta_{lp}, t\right) = \sum_{k=1}^{N_a} d_{klp}\left(\phi_{lp}, \theta_{lp}\right) \cdot b_k \cdot f_k(t), \tag{12}$$

where $d_{klp}\left(\phi_{lp}, \theta_{lp}\right)$ is the complex-valued coefficient of $f_k(t)$ for the direction of arrival path, which could be determined by the direction of the received signal, the structure of the antenna, and the waveforms applied to the antenna. Since the direction can change for each received signal, we assume $d_{klp}\left(\phi_{lp}, \theta_{lp}\right)$ is a random variable, whose amplitude and phase follow a distribution that can be determined by the structure of the antenna and the waveforms applied to the antenna. In discrete time matrix form, Eq. (12) can be shown as $CB\boldsymbol{d}_{lp}$, where

$$B = diag(\boldsymbol{b}) \tag{13}$$

and $diag(\boldsymbol{b})$ is a diagonal matrix whose diagonal components are given by $\boldsymbol{b}$ and $\boldsymbol{d}_{lp} = \left(d_{0lp}\left(\phi_{lp}, \theta_{lp}\right) d_{1lp}\left(\phi_{lp}, \theta_{lp}\right) \ldots d_{(N_c-1)lp}\left(\phi_{lp}, \theta_{lp}\right)\right)^T$.

The receiving process of the proposed MIMO receiver with APM is illustrated in **Figure 2**. We consider that the number of transmit antennas at the transmitter is N_t. Suppose that the channel coefficient is constant during a transmitted symbol. In addition, we assume that the signals transmitted from N_t antennas suffer independent fading. Also, the transmitter is assumed to have no channel state information. Thus, the average transmit power of each transmitted symbol is assumed to be equivalent to each other. When we show the transmitted symbol from the l-th transmit antenna as s_l (**Figure 2**), then, we can have $\mathrm{E}\left[|s_l|^2\right] = 1$ for $l = 1, ..., N_t$ without loss of generality. Besides, the symbol is assumed to be an independent and identically distributed (i.i.d.) random variable. The number of arrival paths per transmit antenna is N_p.

[2] In particular, in the case of the ESPAR antenna, the conversions from the applied voltage to the reactance and from the reactance to the antenna pattern could be nonlinear. Then, the assumption might be optimistic in reality. However, in some cases, we have shown for the conversion from the reactance to the antenna pattern that the effect of the nonlinearity can be suppressed by considering the conversion characteristics [15, 16].

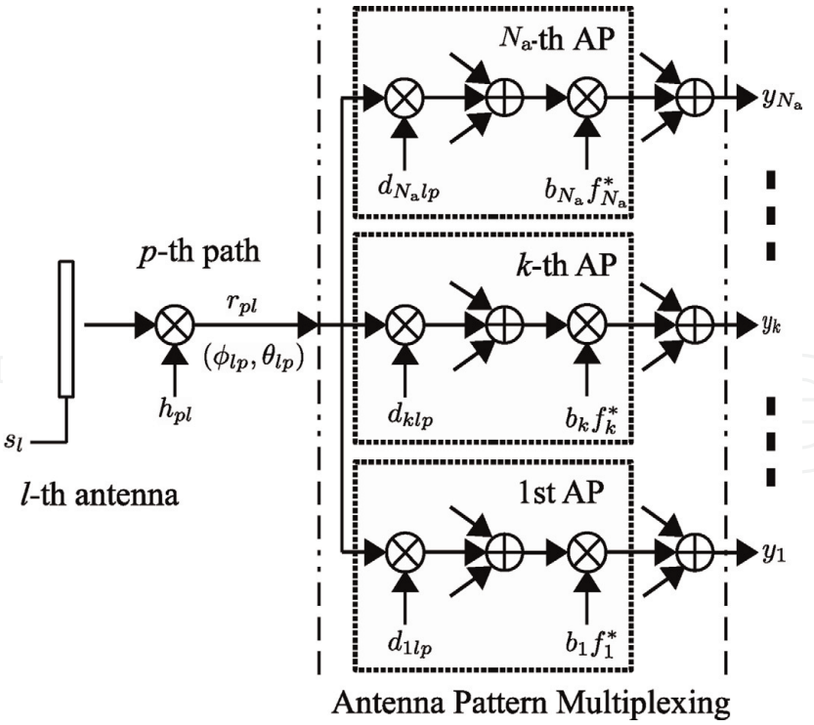


Figure 2.
Receiving process of the receiver with APM.

The p-th path sent from l-th transmit antenna received at the direction of $\left(\phi_{lp}, \theta_{lp}\right)$ is given as follows:

$$r_{pl} = h_{pl} \cdot s_l \tag{14}$$

where h_{pl} means a channel coefficient of a link between the l-th transmit antenna and p-th direction for the antenna and is a complex Gaussian random variable with zero mean and variance of unity.

Now we consider the received signals from N_t transmit antennas. Since N_p paths per transmit antenna arrive at the receiver, the output from the antenna with APM can be shown as follows:

$$x(t) = \sum_{l=1}^{N_t} \sum_{p=1}^{N_p} d_{lp}\left(\phi_{lp}, \theta_{lp}, t\right) \cdot r_{pl} + n(t) \tag{15}$$

$$= \sum_{l=1}^{N_t} \sum_{p=1}^{N_p} \sum_{k=1}^{N_a} d_{klp}\left(\phi_{lp}, \theta_{lp}\right) \cdot b_k \cdot f_k(t) \cdot h_{pl} \cdot s_l + n(t) \tag{16}$$

where $n(t)$ is an additive white Gaussian noise (AWGN) component. As shown in **Figure 2**, the received signal r_{pl} is multiplied by N_a multiplexed antenna patterns $d_{klp}\left(\phi_{lp}, \theta_{lp}\right)$. Since N_p paths are transmitted from the transmit antenna and antenna patterns are orthogonal to each other, the received components for N_p paths are added in each antenna pattern domain separately.

Replacing $x(t)$ with the corresponding vector $\mathbf{x}$, we have the received signal in matrix form as

$$\boldsymbol{x} = \sum_{l=1}^{N_t} \sum_{p=1}^{N_p} CB\boldsymbol{d}_{lp} h_{pl} s_l + \boldsymbol{n} \tag{17}$$

$$= \sum_{l=1}^{N_t} CBD_l \boldsymbol{h}_l s_l + \boldsymbol{n} \tag{18}$$

where D_l is an antenna pattern matrix for l-th transmitted symbol whose size is $N_a \times N_p$ and is given as

$$D_l = \begin{pmatrix} \boldsymbol{d}_{l1} & \boldsymbol{d}_{l2} & \dots & \boldsymbol{d}_{lN_p} \end{pmatrix}, \tag{19}$$

and $\boldsymbol{h}_l$ shows a channel vector whose length is N_p and can be given as

$$\boldsymbol{h}_l = \begin{pmatrix} h_{1l} & h_{2l} & \dots & h_{N_p l} \end{pmatrix}^T, \tag{20}$$

and $\boldsymbol{n}$ is a noise vector whose length is N_c and whose element n_k is an i.i.d. white Gaussian random variable with zero mean and variance σ_n^2/N_c. Then, the autocorrelation matrix of $\boldsymbol{n}$ can be defined as follows:

$$\mathrm{E}\left[\boldsymbol{n}\boldsymbol{n}^H\right] = \frac{\sigma_n^2}{N_c} I_{N_c} \tag{21}$$

Eq. (18) can be further simplified as

$$\boldsymbol{x} = CBDH\boldsymbol{s} + \boldsymbol{n}, \tag{22}$$

by introducing the antenna pattern matrix D defined as

$$D = \begin{pmatrix} D_1 & D_2 & \dots & D_{N_t} \end{pmatrix}, \tag{23}$$

and the channel matrix H, which is a block matrix of $\boldsymbol{h}_l$, defined as

$$H = \begin{pmatrix} \boldsymbol{h}_1 & \boldsymbol{0} & \dots & \boldsymbol{0} \\ \boldsymbol{0} & \boldsymbol{h}_2 & \ddots & \vdots \\ \vdots & \ddots & \ddots & \boldsymbol{0} \\ \boldsymbol{0} & \dots & \boldsymbol{0} & \boldsymbol{h}_{N_t} \end{pmatrix}, \tag{24}$$

where $\boldsymbol{0}$ is a zero and column vector of length N_p and $\boldsymbol{s}$ is a vector of transmitted symbols defined as

$$\boldsymbol{s} = \begin{pmatrix} s_1 & s_2 & \dots & s_{N_t} \end{pmatrix}^T, \tag{25}$$

and its autocorrelation function is given as follows from the assumption:

$$\mathrm{E}\left[\boldsymbol{s}\boldsymbol{s}^H\right] = I_{N_t} \tag{26}$$

The output signal $\boldsymbol{x}$ of the antenna is multiplied by the complex conjugate of the applied waveform. This signal process can be achieved by multiplying $B^{-1}C^H$ by $\boldsymbol{x}$ from the left-hand side, that is, from Eq. (22) to Eq. (11) as

$$\boldsymbol{y} = B^{-1}C^H\boldsymbol{x} \tag{27}$$

$$= B^{-1}C^H(CBDH\boldsymbol{s} + \boldsymbol{n}) \tag{28}$$

$$= B^{-1}C^{\mathrm{H}}CBDH\mathbf{s} + B^{-1}C^{\mathrm{H}}\mathbf{n} \tag{29}$$

$$= DH\boldsymbol{s} + \boldsymbol{n}' \tag{30}$$

where $\boldsymbol{n}' = B^{-1}C^{\mathrm{H}}\boldsymbol{n}$. The autocorrelation matrix of $\boldsymbol{n}'$ can be derived as follows;

$$\mathrm{E}\left[\boldsymbol{n}'\boldsymbol{n}'^{\mathrm{H}}\right] = \mathrm{E}\left[B^{-1}C^{\mathrm{H}}\boldsymbol{n}\left(B^{-1}C^{\mathrm{H}}\boldsymbol{n}\right)^{\mathrm{H}}\right] \tag{31}$$

$$= \mathrm{E}\left[B^{-1}C^{\mathrm{H}}\boldsymbol{n}\boldsymbol{n}^{\mathrm{H}}CB^{-1\mathrm{H}}\right] \tag{32}$$

Here, since the code set C and the matrix B are fixed, and from Eq. (21), we have

$$\mathrm{E}\left[\boldsymbol{n}'\boldsymbol{n}'^{\mathrm{H}}\right] = B^{-1}C^{\mathrm{H}}\mathrm{E}\left[\boldsymbol{n}\boldsymbol{n}^{\mathrm{H}}\right]CB^{-1\mathrm{H}} \tag{33}$$

$$= \frac{\sigma_n^2}{N_{\mathrm{c}}}B^{-1}C^{\mathrm{H}}CB^{-1\mathrm{H}} \tag{34}$$

$$= \frac{\sigma_n^2}{N_{\mathrm{c}}}B^{-1}B^{-1\mathrm{H}} \tag{35}$$

where B^{-1} is a diagonal matrix because B is a diagonal matrix. If we use b_k whose absolute value is unity as $|b_k| = 1$, the k-th diagonal element of B^{-1} is b_k^*. Therefore, we can derive the relation $B^{-1\mathrm{H}} = B$. With the relation between $B^{-1\mathrm{H}}$ and B, we can modify Eq. (35) as

$$\mathrm{E}\left[\boldsymbol{n}'\boldsymbol{n}'^{\mathrm{H}}\right] = \frac{\sigma_n^2}{N_{\mathrm{c}}}B^{-1}B^{-1\mathrm{H}} \tag{36}$$

$$= \frac{\sigma_n^2}{N_{\mathrm{c}}}B^{-1}B \tag{37}$$

$$= \frac{\sigma_n^2}{N_{\mathrm{c}}}I_{N_{\mathrm{c}}}. \tag{38}$$

Thus, the autocorrelation matrix of $\boldsymbol{n}'$ is equivalent to that of $\boldsymbol{n}$.

The process of Eq. (27) can be implemented by multiplying $b_k f_k(t)$ by $x(t)$ in parallel and integrating them over the interval T_{s} or with a correlator as shown in **Figure 2**. Since N_{t} transmit antennas are assumed, N_{t} components are added in each antenna pattern domain. Note that the process divides a single signal output into N_{a} outputs or N_{a} antenna pattern domains.

If we recognise the matrix DH in Eq. (30) as an equivalent channel matrix $G = DH$ that is equivalent to that of the conventional MIMO systems, we can rewrite Eq. (30) as

$$\boldsymbol{y} = G\boldsymbol{s} + \boldsymbol{n}' \tag{39}$$

Since the length of $\boldsymbol{y}$ is N_{a}, the proposed MIMO with APM seems equivalent to conventional $N_{\mathrm{t}} \times N_{\mathrm{a}}$ MIMO systems [19]. The number N_{a} shows the number of orthogonal antenna patterns in time domain[3]. However, the number corresponds to the number of virtual receive antennas in the context of MIMO receivers. The

[3] The orthogonality in time domain does not guarantee the orthogonality in space domain or in terms of directivity. It is a challenging problem to develop a set of orthogonal functions in both time and space domains.

equation above realises that the received components obtained by the receiver with APM are similar to those of the conventional MIMO systems. We assume that the receiver has perfect knowledge of the equivalent channel matrix G. Note that the receiver does not need to know every element of D or H for decoding. In practice, it may even be impossible to separately evaluate the components of D and H.

3.3 Capacity of MIMO systems with APM

From the received signal in Eq. (39) and the autocorrelation matrix of the transmitted symbols in Eq. (26), we can derive the ergodic capacity C[4] as

$$C = \mathrm{E}\left[\log_2 det\left(I_{N_\mathrm{t}} + \frac{\gamma}{N_\mathrm{t}} G^\mathrm{H} G\right)\right] \tag{40}$$

where *det* is the determinant of a matrix and γ is the average signal-to-noise ratio (SNR) per transmit antenna and is defined as $\gamma = 1/\sigma_n^2$. As we can see from Eq. (40), the capacity depends on the property of the equivalent channel matrix G or DH. Here, the matrix G satisfies the following properties which are similar to the channel matrix of the conventional MIMO systems:

$$\mathrm{E}\left[GG^\mathrm{H}\right] = N_\mathrm{t} I_{N_\mathrm{a}}, \tag{41}$$

$$\mathrm{E}\left[G^\mathrm{H} G\right] = N_\mathrm{a} I_{N_\mathrm{t}} \tag{42}$$

4. Numerical results

In this section, we show the ergodic capacity of a MIMO system whose receiver uses the proposed APM technique. Through the section the number of transmit antennas is $N_\mathrm{t} = 2$. The capacity C (40) of the proposed MIMO system is shown in **Figure 3**. We assume that the coefficients of the matrix D are denoted as $\exp(j\Theta)/\sqrt{N_\mathrm{p}}$ where Θ is a uniform random variable in the interval $[0, 2\pi)$. In the figure, the number of antenna patterns or virtual antenna outputs $N_\mathrm{a} = 8$. If the channel coefficient is constant while a symbol is transmitted, the code set satisfying Eq. (11) could not affect on the performance. Thus, we do not specify the code set in this study. We evaluate the capacities for the number of arrival paths $N_\mathrm{p} = 1$, 2, 4, 8, 16, and 32 and show them with solid lines. For comparison, we also show the ergodic capacity of the conventional MIMO systems with black dashed lines marked with dots ('·'). The pairs of transmit and receive antennas are 2×1 MIMO and 2×2 MIMO systems.

The capacities of the MIMO systems with APM are between those of the conventional 2×1 and 2×2 MIMO systems. In lower SNR region, the capacity of MIMO with APM for various N_p is close to that of the conventional 2×1 MIMO. On the other hand, in higher SNR region, the values and also the slopes of the capacities converge to those of the conventional 2×2 MIMO. When the number of arrival paths N_p increases, the capacities also increased and converged towards the capacity of the conventional 2×2 MIMO system. Since the slope of the capacity relates to diversity order, the proposed APM technique can achieve the same order as the conventional 2×2 MIMO systems even if $N_\mathrm{p} = 1$. Because of the increased

[4] We use the same variable character as code matrix. Since they are used in different contexts, they might be easily distinguishable.

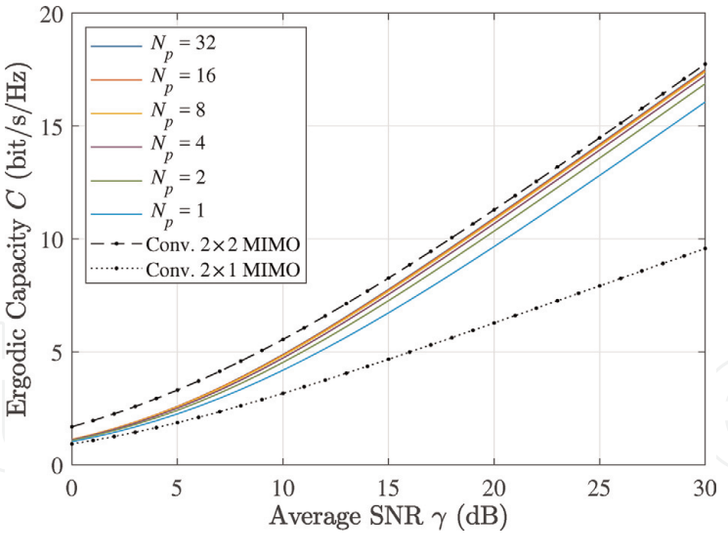


Figure 3.
Ergodic capacity of MIMO systems with APM technique versus average SNR for various number of arrival paths N_p. ($N_t = 2$, $N_a = 8$).

capacity due to the increase in the number of arrival paths, it can be recognised that the proposed APM obtains path diversity gain. As mentioned in Section 2, APM technique can reduce the antenna size and hardware cost. Thus, we can find that the proposed technique can provide similar capacities with reduced size and less hardware cost.

We show the ergodic capacities versus average SNR of the proposed MIMO systems with APM for fixed number of arrival paths $N_\mathrm{p} = 16$ and various number of antenna patterns, i.e., $N_\mathrm{a} = 1$, 2, 4, 8, and 16, in **Figure 4**. The number $N_\mathrm{p} = 16$ might be sufficiently large to obtain the path diversity gain according to **Figure 3**. For comparison purposes, the performances of the conventional 2×1 and 2×2 MIMO systems are also drawn.

The capacities for APM techniques increase in the number of antenna patterns N_a and converge to those of the conventional 2×1 MIMO systems in lower SNR region and the 2×2 MIMO systems in higher SNR region. When $N_\mathrm{a} = 16$, the capacity almost overlaps the capacity of the conventional 2×2 MIMO systems in the region average SNR, which is more than 20 dB. In the case $N_\mathrm{a} = 1$, the capacity

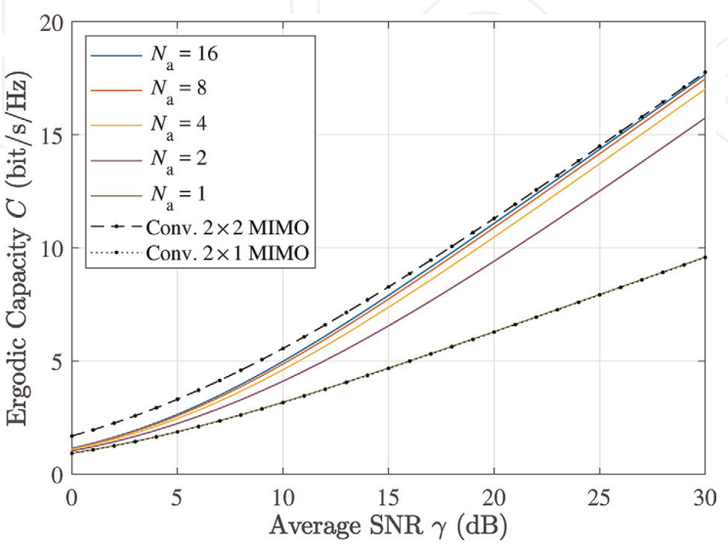


Figure 4.
Ergodic capacity of MIMO systems using receiver with APM technique for various number of orthogonal antenna patterns. Antenna pattern matrix has constant amplitude and random phase with uniform distribution. ($N_t = 2$, $N_p = 16$).

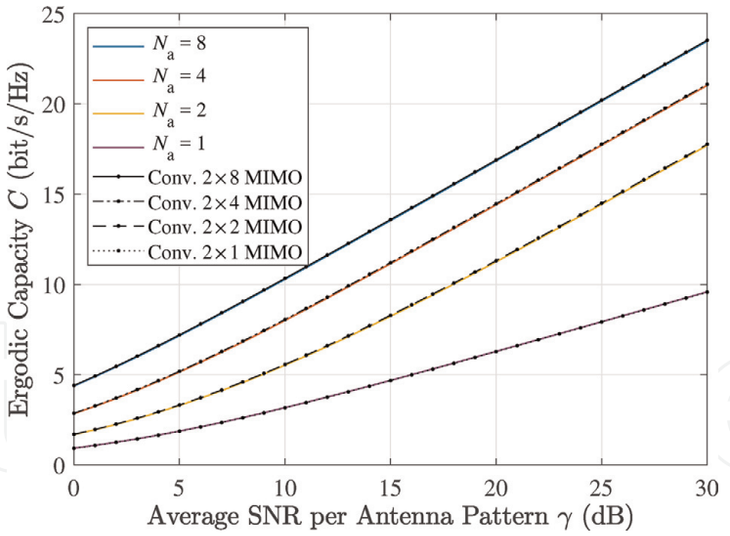


Figure 5.
Ergodic capacity of MIMO systems with APM technique for various number of orthogonal antenna patterns. Average SNR per antenna pattern is a constant ($N_t = 2$, $N_p = 16$).

of the proposed MIMO systems with APM is equivalent to that of the conventional 2×1 MIMO system. Hence, diversity gain cannot be obtained even if the number of arrival paths is sufficiently large.

Then we consider the case that the average SNR per antenna pattern or virtual antenna is given as γ. In this case, the coefficients in the matrix D are random variables shown as $\exp(j\Theta)$ where Θ is a uniform random variable in the interval $[0, 2\pi)$. The ergodic capacities of the proposed MIMO systems with APM are shown for $N_a = 1$, 2, 4, and 8 for $N_p = 16$ in **Figure 5**. In the figure, we also illustrate the capacities of the conventional MIMO systems for 2×1, 2×2, 2×4, and 2×8 in terms of the numbers of transmit and receive antennas. As we can see from the figure, the capacities are equivalent to each other between N_a for APM and the same number of receive antennas for the conventional MIMO. For example, when $N_a = 8$, the capacity is the same as that of 2×8 MIMO systems. Therefore, when the average SNR per antenna pattern is same as the average SNR per the number of receive antennas, the proposed APM-based MIMO systems with N_a antenna patterns achieve almost equivalent capacity to the conventional $N_t \times N_a$ MIMO systems.

5. Conclusions

In this chapter we propose a concept of APM for MIMO receiver to reduce the antenna size and hardware cost with keeping the availability of diversity gain. We discuss the types of antennas which achieve the APM, i.e., generating time-varying antenna pattern. Also, we discuss the benefits of the antennas, in particular, for ESPAR antenna-based structure. The number of virtual antennas or antenna patterns can be increased with the number of multiplexed orthogonal signals used to change the antenna patterns. A model of receiving process is proposed for analysing the capacity of systems using APM. We derive a model of received signals to analyse the system performance. The received signal in matrix form includes an equivalent channel matrix, which is a product of antenna pattern matrix, the channel coefficient vector for each output.

When the number of arrival paths and the number of antenna pattern are sufficiently large, the ergodic capacity approaches to that of 2×2 MIMO systems.

The property deduces the proposed APM, which can obtain diversity gain from path diversity and diversity reception based on the virtual antennas.

On the other hand, numerical results show that the ergodic capacity is equivalent to that of the conventional MIMO systems when the average SNR per antenna pattern is constant. Then, the proposed APM-based receiver can exploit path diversity gain and antenna pattern diversity maximally without additional physical antenna elements.

Future work is a development of efficient multiplexed antenna patterns, which have larger number of orthogonal antenna patterns than the number of antenna elements equipped with a cable.

Acknowledgements

This work was carried out by the joint usage/research programme of the Institute of Materials and Systems for Sustainability (IMaSS), Nagoya University.

Abbreviations

AP	antenna pattern
APM	antenna pattern multiplexing
CDM	code-division multiplexing
CDMA	code-division multiple access
DS/SS	direct-sequence spread spectrum
ESPAR	electronically steerable passive array radiator
i.i.d.	independent and identically distributed
MIMO	multiple-input multiple-output
MISO	multiple-input single-output
MSE	modulated scattering element
OFDM	orthogonal frequency-division multiplexing
PSK	phase-shift keying
QAM	quadrature amplitude modulation
RF	radio frequency
SIMO	single-input multiple-output
SINR	signal-to-interference-plus-noise ratio
SISO	single-input single-output
SNR	signal-to-noise ratio
VRE	variable reactance element

IntechOpen

IntechOpen

Author details

Masato Saito
Faculty of Engineering, University of the Ryukyus, Nishihara, Japan

*Address all correspondence to: massai@ieee.org

IntechOpen

© 2019 The Author(s). Licensee IntechOpen. This chapter is distributed under the terms of the Creative Commons Attribution License (http://creativecommons.org/licenses/by/3.0), which permits unrestricted use, distribution, and reproduction in any medium, provided the original work is properly cited. CC BY

References

[1] Ohira T, Gyoda K. Electronically steerable passive array radiator antennas for low-cost analog adaptive beamforming. In: Proceedings 2000 IEEE International Conference on Phased Array Systems and Technology (Cat. No.00TH8510). 2000. pp. 101-104. DOI: 10.1109/PAST.2000.858918

[2] Chen Q, Takeda Y, Yuan Q, Sawaya K. Diversity performance of modulated scattering array antenna. IEICE Electronics Express. 2007;**4**(7): 216-220. DOI: 10.1587/elex.4.216

[3] Chen Q, Wang L, Iwaki T, Kakinuma Y, Yuan Q, Sawaya K. Modulated scattering array antenna for MIMO applications. IEICE Electronics Express. 2007;**4**(23):745-749. DOI: 10.1587/elex.4.745

[4] Wang L, Chen Q, Yuan Q, Sawaya K. Diversity performance of modulated scattering antenna array with switched reflector. IEICE Electronics Express. 2010;**7**(10):728-731. DOI: 10.1587/elex.7.728

[5] Wang L, Chen Q, Yuan Q, Sawaya K. Numerical analysis on MIMO performance of the modulated scattering antenna array in indoor environment. IEICE Transactions on Communications. 2011;**E94–B**: 1752-1756. DOI: 10.1587/transcom.E94.B.1752

[6] Yuan Q, Ishizu M, Chen Q, Sawaya K. Modulated scattering array antenna for mobile handset. IEICE Electronics Express. 2005;**2**(20): 519-522. DOI: 10.1587/elex.4.745

[7] Bains R, Muller R. Using parasitic elements for implementing the rotating antenna for mimo receivers. IEEE Transactions on Wireless Communications. 2008;**7**:4522-4533. DOI: 10.1109/T-WC.2008.060808

[8] Kalis A, Kanatas AG, Papadias CB, editors. Parasitic Antenna Arrays for Wireless MIMO Systems. New York: Springer-Verlag; 2014. DOI: 10.1007/978-1-4614-7999-4

[9] Reinoso Chisaguano DJ, Hou Y, Higashino T, Okada M. Low-complexity channel estimation and detection for mimo-ofdm receiver with espar antenna. IEEE Transactions on Vehicular Technology. 2016;**65**: 8297-8308. DOI: 10.1109/TVT.2015.2506782

[10] Arita W, Saito M. Novel receive diversity scheme using espar antenna and arbitrary frequency band. In: 2012 IEEE Vehicular Technology Conference (VTC Fall). 2012. pp. 1-5. DOI: 10.1109/VTCFall.2012.6399283

[11] Dia A, Saito M. A study on channel capacity of mimo systems with a receiver with antenna pattern modulation. In: 2017 International Symposium on Antennas and Propagation (ISAP). 2017. DOI: 10.1109/ISANP.2017.8228953

[12] Idoguchi Y, Saito M. Evaluation of antenna with periodically variable directivity. In: 2014 Asia-Pacific Microwave Conference. 2014. pp. 345-347

[13] Idoguchi Y, Saito M. A study on received signal spectrum of antenna with periodically variable directivity. In: 2014 International Symposium on Antennas and Propagation Conference Proceedings. 2014. pp. 403-404

[14] Saito M. A study on mimo systems with antenna pattern modulation technique. In: IEICE Tech. Rep. 2017. pp. 51-56. (in Japanese)

[15] Kawano K, Idoguchi Y, Saito M. Evaluation of power spectrum of 2-element dipole antenna with

periodically variable antenna pattern. In: 2016 International Symposium on Antennas and Propagation (ISAP). 2016. pp. 412-413

[16] Kawano K, Saito M. Periodic reactance time functions for 2-element espar antennas applied to 2-output simo/mimo receivers. IEICE Transactions on Communications. 2019; **E102.B**(4):930-939. DOI: 10.1587/transcom.2018EBP3097

[17] Saito M. Periodically variable antenna pattern for maximizing path diversity gain in mimo receivers. In: 2018 5th IEEE Uttar Pradesh Section International Conference on Electrical, Electronics and Computer Engineering (UPCON). 2018. pp. 1-6. DOI: 10.1109/UPCON.2018.8597063

[18] Sun C, Hirata A, Ohira T, Karmakar NC. Fast beamforming of electronically steerable parasitic array radiator antennas: Theory and experiment. IEEE Transactions on Antennas and Propagation. 2004;**52**(7): 1819-1832. DOI: 10.1109/TAP.2004.831314

[19] Proakis JG, Salehi M. Digital Communications. 5th ed. Boston: McGraw-Hill Education; 2007